JOURNAL OF MATERIALS SCIENCE 39 (2004) 6325–6331

Crystallization and structural properties of calcium malonate hydrate

P. A. VARUGHESE*, K. V. SABAN, J. GEORGE, I. PAUL, G. VARGHESE
Crystal Physics Centre, St. Berchmans' College, Changanacherry 686 101, Kerala, India
E-mail: gvarghese@sancharnet.in

Calcium malonate hydrate crystals were grown by the reaction method, with the aid of hydrosilica gel. Colourless and prismatic crystals up to 4.5 mm in size were obtained. Structural properties of the material were explored by employing X-ray diffraction (XRD), infrared (IR) absorption, laser Raman (LR), and thermogravimetric (TG) techniques. The IR spectrum indicates the presence of inequivalent water molecules in the structure of the compound. The thermal decomposition pattern of the sample suggests a three-stage decay scheme. About one-fifth of the weight is due to the presence of water of crystallization. The differential scanning calorimetric (DSC) study corroborates the presence of inequivalent water molecules in the structure.

1. Introduction

Extensive study on the crystallization and properties of oxalates and tartrates of alkaline earth metals has been made by many investigators [1–6]. However, less attention was given by crystal growers to the malonates of these metals. Malonates are salts of malonic acid; the next higher homologue of oxalic acid. The malonate ligand is characterized by a fairly active methylene group ($-CH_2$) between two carboxylate groups. There has been intense recent interest in the binding modes of calcium ion to carboxylate and especially dicarboxylate ions because of the significance of such interactions in the blood and bone proteins containing the modified amino acid residues γ-carboxyglutamic acid (Gla) and β-carboxyaspartic acid (Asa) [7–12].

Alkaline earth metal carboxylates and their decomposition products find wide applications in industry as pharmaceuticals, catalysts, ceramics, glasses etc., hence their decomposition study has become a subject of interest [13]. This paper reports the growth of calcium malonate hydrate crystals by the gel-aided solution technique. Here a gel column enriched with the anions promotes the growth process by the controlled supply of these ions to the supernatant solution, containing the cations and the crystals form and grow in the solution. Optimum conditions for the growth at ambient temperature were found by investigating different growth parameters. The crystals were characterized by the physico-chemical probes of investigation such as chemical, X-ray and spectroscopic methods. Thermal decomposition pattern of the sample was analysed by TG and DSC techniques, which exhibits interesting decomposition scheme.

2. Experimental

Crystallization of the title compound ($CaC_3H_2O_4 \cdot 2H_2O$) was achieved with the help of hydrosilica gel [14–16]. Reagent grade sodium metasilicate powder was dissolved in double distilled water and the resultant solution was filtered out. The specific gravity of this solution was maintained at 1.025 and was titrated with 1 M malonic acid (Analar Grade) to obtain a pH value 7. The resultant mixture was taken in glass tubes of internal diameter 18 mm and length 150 mm and kept idle for gelation. Firm gel columns were obtained inside the tubes within 24 h. Over the set gel, 0.2 M calcium chloride (Analar Grade) was carefully poured as the supernatant solution that provides calcium ions for the onset of the chemical reaction:

$$H_4C_3O_4 + CaCl_2 + 2H_2O \rightarrow CaC_3H_2O_4 \cdot 2H_2O + 2HCl$$

The gelatinous medium present here, in fact, controls the diffusion process. Small crystals appeared in the supernatant solution, near the gel-solution interface, within 48 h. Regular observation of these crystals showed that they grew to the maximum size of 4.5 mm in 3–4 weeks. No crystal was formed inside the gel medium. The experiment was repeated by altering the parameters such as concentrations of the nutrients, pH, density and age of the gel medium. The concentration of malonic acid was varied from 0.5–2.0 M and that of calcium chloride from 0.1–0.3 M to observe noticeable changes in the crystallization. Gel media having different specific gravities (1.02, 1.025, 1.03, 1.035, 1.04, and 1.05), pH values (4, 5, 6, 7, 8 and 9)

*Present address: Department of Physics, St. Michael's College, Cherthala 688 539, Kerala, India.

TABLE I Conditions of crystal growth by the gel-aided solution technique and the nature of growth

Sp. gravity of gel	pH	Conc. of $H_4C_3O_4$ and $CaCl_2$	Number of crystals	Average size (mm)	Nature of growth
1.03	4	1 M, 0.2 M	8	–	Few twinned crystals, less transparent.
1.03	5	1 M, 0.2 M	6	–	Few twinned crystals, less transparent.
1.03	6	1 M, 0.2 M	3	4	Prismatic, faceted and transparent.
1.03	7	1 M, 0.2 M	3	4	Prismatic, faceted and transparent.
1.03	8	1 M, 0.2 M	7	–	Few crystals have interlaced growth.
1.03	9	1 M, 0.2 M	8	–	Interlaced growth
1.020	7	1 M, 0.2 M	2	3	Prismatic, faceted and transparent.
1.025	7	1 M, 0.2 M	2	4.5	Prismatic, faceted and transparent.
1.030	7	1 M, 0.2 M	3	3	Prismatic, faceted and transparent.
1.035	7	1 M, 0.2 M	7	2	Prismatic, but less transparent
1.040	7	1 M, 0.2 M	7	–	Crystals formed at the interface grew into the gel with interlaced growth.
1.050	7	1 M, 0.2 M	11	–	Crystals formed at the interface grew into the gel with interlaced growth.
1.025	7	0.5 M, 0.2 M	2	3	Transparent, faceted, prismatic crystals.
1.025	7	1.5 M, 0.2 M	8	–	Few crystal aggregates with rough surfaces.
1.025	7	2.0 M, 0.2 M	12	–	Crystal aggregates with rough surfaces
1.025	7	1 M, 0.10 M	1	3	Transparent, faceted, prismatic crystals.
1.025	7	1 M, 0.15 M	2	3	Transparent, faceted, prismatic crystals.
1.025	7	1 M, 0.25 M	4	–	Few crystal aggregates with rough surfaces.
1.025	7	1 M, 0.30 M	6	–	Crystal aggregates with rough surfaces.

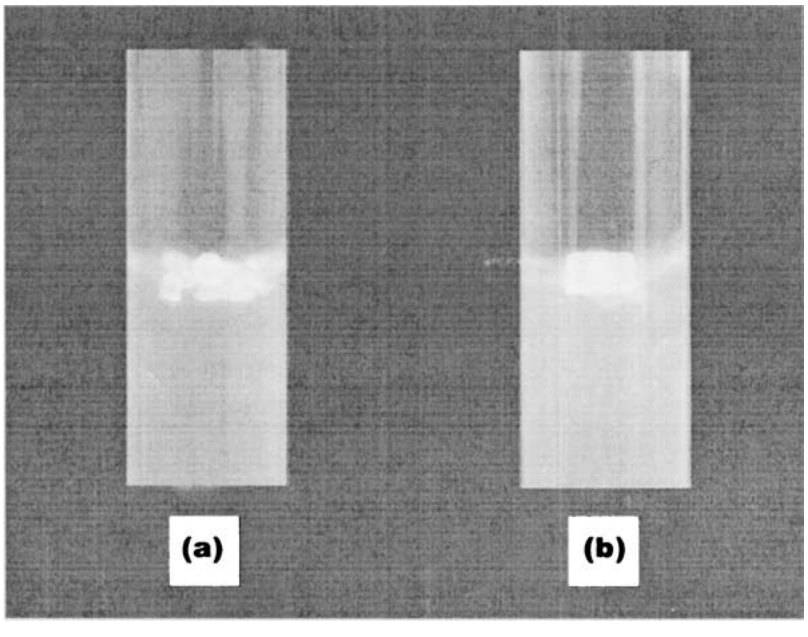

Figure 1 Tubes containing crystals formed under two different growth conditions: (a) silica gel of specific gravity 1.03, pH $\sim$ 8, outer electrolyte $CaCl_2$ – 0.2 M, inner electrolyte, $H_4C_3O_4$ – 1 M, (b) silica gel of specific gravity 1.025, pH $\sim$ 7, outer electrolyte $CaCl_2$ – 0.2 M, inner electrolyte $H_4C_3O_4$ – 1 M.

and age (1, 2, 3, 4, 5, and 6 days) were tried in the set of experiments. All the major observations are compiled in Table I. Crystallization tubes containing crystals formed under two different growth conditions are depicted in Fig. 1.

Combustion analysis was carried out for detecting the presence of carbon (C) and hydrogen (H) and atomic absorption for calcium (Ca) in the sample. X-ray diffraction pattern of the powdered sample was obtained using Philips 1710 X-ray generator with Ni filtered Cu K_α radiation. The pattern was recorded at a scan speed of 1° per minute. Fourier transform infrared (FT-IR) absorption spectrum of the sample was recorded using Bruker IFS 66 V spectrometer, in the wavenumber range 4000–400 cm^{-1}, using the KBr pellet technique. The spectral resolution of the instrument was 0.1 cm^{-1}. Dilor Z 24 Laser Raman spectrometer having a resolution 0.5 cm^{-1} was used to scan the Raman spectrum of the sample, using an excitation wavelength of 647.1 nm. Thermogravimetric runs were taken on a Metler TA 4000 system. The TG-DTG and DSC patterns were obtained using 8.398 and 4.557 mg samples respectively by scanning at the rate of 10°C per minute, under oxygen atmosphere.

3. Results and discussion

Nucleation and growth of crystals of the compound occurred in the upper solution, near the gel-solution interface. A few crystals obtained are shown in Fig. 2. When the gel medium had pH values 6 and 7, more or less transparent, prismatic and faceted crystals, with a

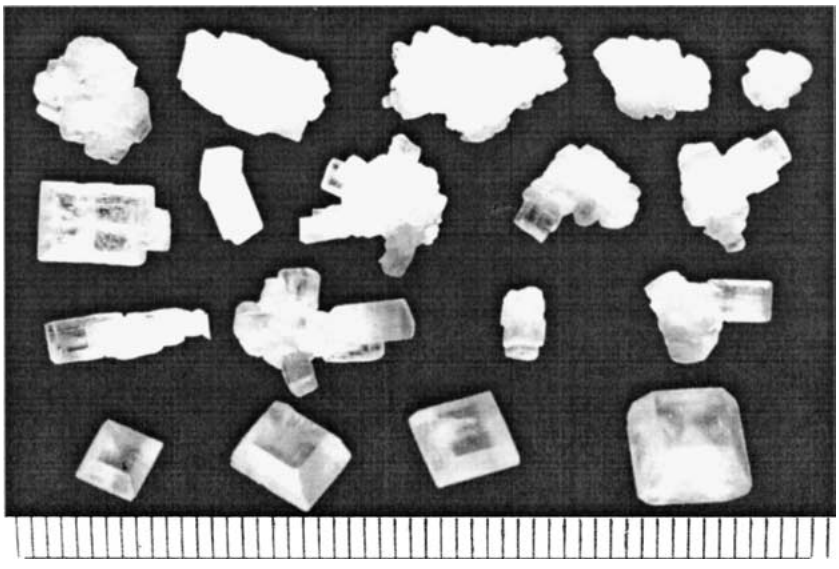

Figure 2 Different morphologies of calcium malonate hydrate crystals grown by the gel-aided solution technique.

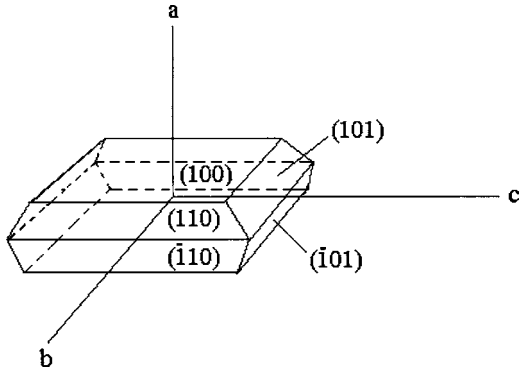

Figure 3 Schematic illustration of the habit of calcium malonate hydrate crystals.

well-defined habit (Fig. 3), were obtained. More crystals were found to grow with smaller size when the pH value was less than 6. At lower pH, the medium is more acidic and the supply of malonate ions into the upper solution may be high. This may be a possible reason for the higher nucleation rate in the lower pH regime. The size reduction may be due to the greater number of nucleation centres and the consequent competition between the nuclei for the solute particles [17]. When the pH value was above 7, more number of crystals, with a few having interlaced growth, was obtained. As the pH increases, the box-like network structure of the gel changes to a loosely bound platelet structure, which lacks cross-linkages [17]. This may enhance the number of malonate ions diffusing upwards, resulting in an increased number of nucleation centres in the supernatant solution.

With low dense gel (specific gravity $\leq$1.03), more transparent and faceted crystals were obtained. For higher gel densities (specific gravity $\geq$1.04), the crystals formed over the gel surface were found to protrude into the gel. When the gel density was high enough, the diffusion rate of malonate ions in the upward direction may be less than that of calcium ions in the downward direction. The probable meeting point of the two ions may be inside the gel. The nucleated particles then flocculate to the lower ends of the crystals at the interface.

The concentration of the reactants was found to influence the rate of growth of the crystals. The number of nucleation centres was found to increase with the concentration of the nutrients. When the concentration of $CaCl_2$ was above 0.2 M, more or less opaque crystal aggregates with rough surfaces and irregular morphology were obtained. This may be due to the increase in growth rate and the inclusion of impurities. More transparent, prismatic and faceted crystals were formed when the concentration of $CaCl_2$ was less than or equal to 0.2 M. But the number and size of the crystals formed was found to decrease with decrease in the concentration. This can be attributed to the decreased number of growth units available at lower concentrations. When the malonic acid concentration was less than or equal to 1 M, faceted prismatic crystals were obtained. But higher concentrations resulted in the formation of increased number of crystal aggregates.

Ageing of the gel was found to have practically no influence on the growth of the crystals. The crystals were formed in the upper solution and the gel only controls the diffusion of one of the nutrients. The ageing alone doesn't produce any major change in the diffusion process of malonate ions in this case.

The optimum conditions for the growth of transparent, well faceted, prismatic crystals of maximum size are:

(i) specific gravity of gel = 1.025
(ii) pH of gel medium = 6–7
(iii) concentration of inner reagent = 1 M
(iv) concentration of feed solution = 0.2 M
(v) growth period = 3–4 weeks

Results of the elemental analyses were satisfactory. The percentages of the elements were found to be in agreement with the calculated values (Table II).

3.1. X-ray diffraction

XRD pattern of the powdered sample is shown in Fig. 4. The well-defined Bragg peaks at specific 2θ angles

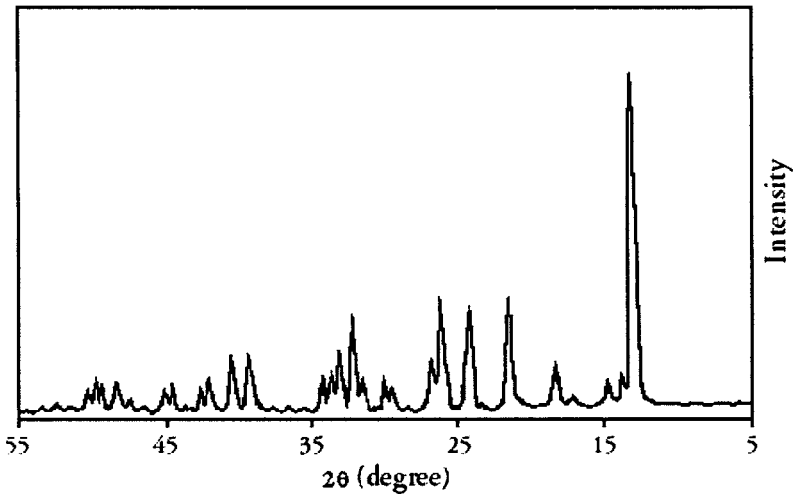

Figure 4 X-ray diffractogram of calcium malonate hydrate.

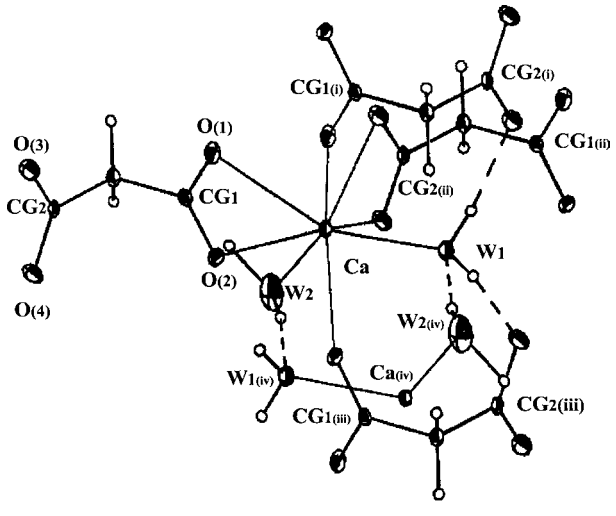

Figure 5 View of the coordination of the different groups to Ca in $CaC_3H_2O_4 \cdot 2H_2O$.

TABLE III X-ray powder diffraction data for calcium malonate hydrate

2θ (deg)	d_{obs} (Å)	d_{std} (Å)	I/I_0	*hkl*
13.2	6.7019	6.6570	100	200
18.6	4.7666	4.7570	13	−111
21.4	4.1488	4.1200	33	201
24.4	3.6451	3.6180	31	−311
26.2	3.3986	3.4060	34	020
26.6	3.3484	3.3280	15	400
32.3	2.7693	2.7480	28	−402
33.2	2.6963	2.6770	17	401
33.6	2.6651	2.6520	10	202
34.0	2.6347	2.6250	9	221
39.2	2.2963	2.2830	16	−512
40.4	2.2308	2.2100	15	312
42.0	2.1495	2.1350	9	−602
44.5	2.0343	2.0210	8	330
48.4	1.8791	1.8882	8	−132
50.0	1.8227	1.8264	9	−332

TABLE IV Unit cell parameters of calcium malonate hydrate

Lattice	Monoclinic
Space group	C2/m
Cell dimensions	$a = 13.871$ Å
	$b = 6.812$ Å
	$c = 6.804$ Å
	$\beta = 106.28^\circ$
Volume	617.13 Å^3
Z	4

reveals that the smaple crystallizes in monoclinic system. The observed *d* values and the standard values in the ASTM data card were in close agreement (Table III). Unit cell parameters of the compound are presented in Table IV. The fundamental features of the structure along with the label of the different groups [18] are also depicted (Fig. 5).

3.2. Vibrational spectroscopy

The FT-IR absorption spectrum of the material is shown in Fig. 6 and the corresponding LR spectrum in Fig. 7. According to the structural characteristics of the compound, the internal vibrations are mainly due to carboxylate groups, methylene group and water molecules.

TABLE II Percentages of elements C, H and Ca in calcium malonate hydrate

C (%)		H (%)		Ca (%)	
Found	Calculated	Found	Calculated	Found	Calculated
19.86	20.23	3.06	3.37	21.60	22.51

The spectra are interpreted by comparing with those of malonic acid and related compounds available in the literature [19–21]. The absorption wavelengths and the proposed assignments are presented in Table V.

In the IR spectrum two sets of bands are observed in the water stretching zone. This suggests the presence of crystallographically inequivalent water molecules in the crystal lattice. The lowered wavenumber values for these bands show not only the water coordination to calcium ion but also the presence of hydrogen bonds in the lattice. The bands at the lower wavenumber values (3216 and 3053 cm^{-1}) are attributed to W1 water molecules which are hydrogen bonded to the

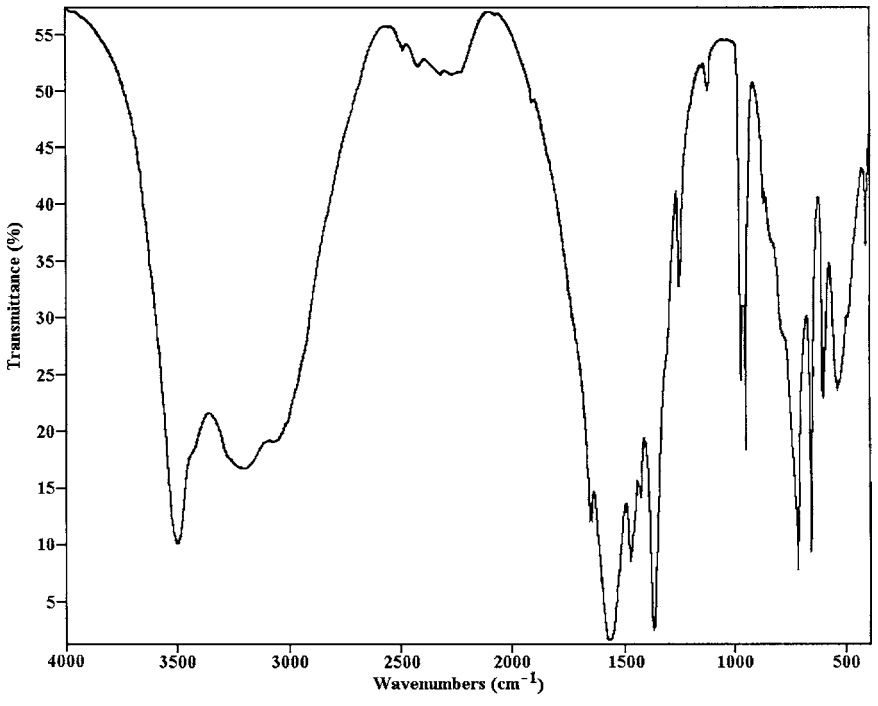

Figure 6 FTIR spectrum of calcium malonate hydrate.

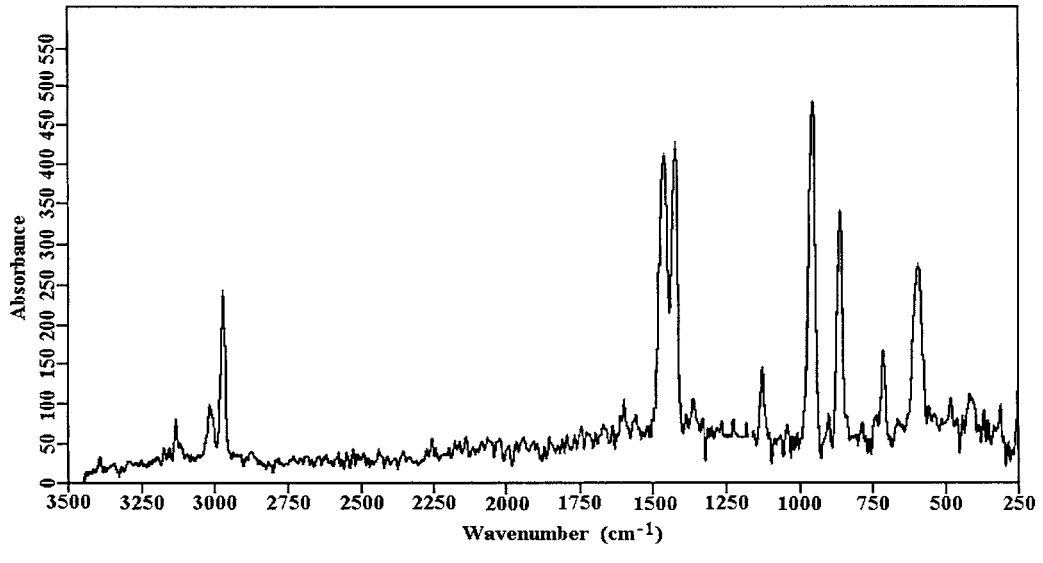

Figure 7 Laser Raman spectrum of calcium malonate hydrate.

carboxylate group CG2 and those at higher wavenumbers (3496 and 3427 cm^{-1}) are ascribed to W2 water molecules which are only hydrogen bonded to W1 (Fig. 5). The dehydration process exhibited in the thermogravimetric studies also supports this assignment. The bands at 1660 and 1665 cm^{-1} appear as a doublet and this may be due to the bending modes of the two inequivalent water molecules. It is seen that two bands (875 and 730 cm^{-1}) appear for the rocking motion of water and this also suggests the presence of two inequivalent water molecules in the crystal [22]. The medium band at 542 cm^{-1} in the spectrum is ascribed to the wagging and twisting modes. The band at 410 cm^{-1} is attributed to the M-OH_2 stretching motion.

The very strong band centred around 1581 cm^{-1} is assigned to the asymmetric stretching of the carboxylate group and the one at 1377 cm^{-1} is ascribed to the symmetric stretching. Both these stretching modes are shifted to lower frequencies as compared to those of free malonate ion in sodium malonate [23] indicating increased coordination bond strength [24]. The Raman spectrum also exhibits a strongly polarized line at 1430 cm^{-1}, which is also characteristic of the symmetric stretching vibration of the carboxylate group.

The bands at 785, 725 and 664 cm^{-1} in the IR spectrum are respectively attributed to the deformation modes δ(OCO), ρ_w(OCO), and π(OCO) of the carboxylate group. A weak band at 716 cm^{-1} is observed in the Raman due to the deformation mode ρ_w(OCO).

The medium band at 603 cm^{-1} in the IR spectrum and the one at 601 cm^{-1} in the Raman spectrum represent the bending mode δ(CCO).

The very weak band at 1128 cm^{-1} in the IR is due to the asymmetric stretch ν_{as}(CC) of the C─C bond [25]

TABLE V Assignment of the vibrational spectra of calcium malonate hydrate

Wavenumber (cm^{-1})		
FTIR	Raman	Assignment
3496 (s)		ν_{as}(OH)-W2
3427 (sh)		ν_{s}(OH)-W2
3216 (br)		ν_{as}(OH)-W1
3053 (sh)		ν_{s}(OH)-W1
	2976 (s)	ν_{s}(CH)
1660–1665 (m)(d)		$\delta(H_2O)$
1581 (vs) (br)		ν_{as}(OCO)
1484 (s)	1470 (s)	$\delta(CH_2)$
1440 (m)		$\delta(CH_2)$
1377 (vs)	1430 (vs)	ν_{s}(OCO)
1260 (w)		$\rho_{w}(CH_2)$
1128 (vw)		ν_{as}(CC)
975 (m)	963 (vs)	ν_{s}(CC)
954 (m)		$\rho_{r}(CH_2)$
875 (vw)		$\rho_{r}(H_2O)$
	865 (s)	δ(CC)
785 (sh)		δ(OCO)
730 (sh)		$\rho_{r}(H_2O)$
725 (s)	716 (m)	ρ_{w}(OCO)
664 (s)		δ(CCO)
603 (m)	601 (m)	δ(OCO)
542 (m)		$\rho_{w}(H_2O) + \rho_{t}(H_2O) + \pi$(CCO)
410 (w)		ν(M-OH_2)

s, strong; sh, shoulder; br, broad; m, medium; d, doublet; vs, very strong; w, weak; vw very weak; ν_{as}, asymmetric stretching; ν_{s}, symmetric stretching; δ, deformation; ρ_{w}, wagging mode; ρ_{r}, rocking mode; π, out of plane deformation; ρ_{t}, twisting mode.

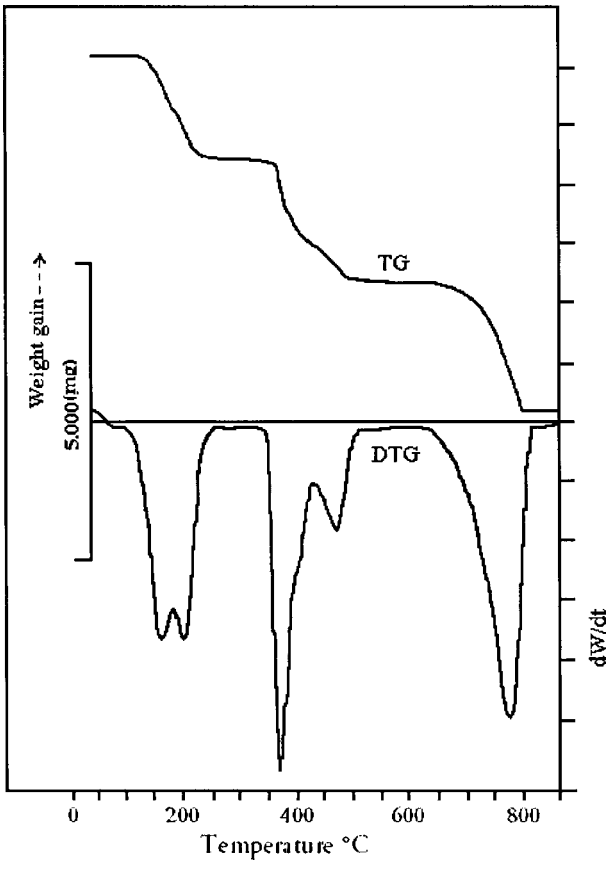

Figure 8 Thermogram showing simultaneous recording of TG and DTG curves for calcium malonate hydrate.

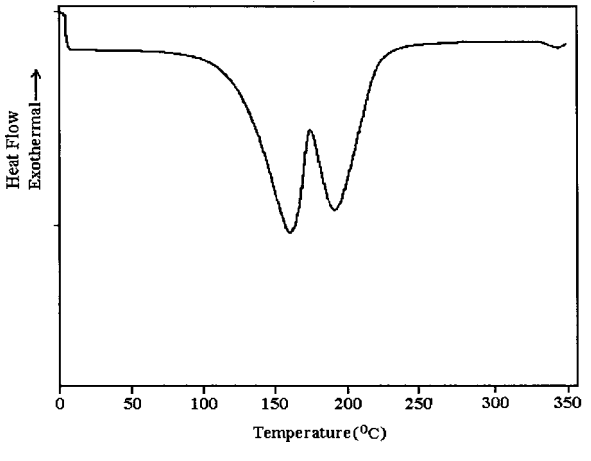

Figure 9 DSC curve recorded for calcium malonate hydrate.

while the band at 975 cm^{-1} is due to the symmetric stretch. Corresponding to the symmetric stretch there is a very intense Raman line at 963 cm^{-1}. There is also an intense Raman line at 865 cm^{-1} due to the δ(CC) mode.

The Raman line at 2976 cm^{-1} is assigned to the symmetric stretching mode ν_{s}(CH). But the band due to the asymmetric stretch ν_{as}(CH) around 2900 cm^{-1} is not evident in the IR spectrum. This may be due to the overlapping of this band with the broad absorption band of water.

In the IR spectrum, two bands are seen at 1484 and 1440 cm^{-1}. They are attributed to the bending modes of methylene group $\delta(CH_2)$. The Raman spectrum also shows a very intense line at 1470 cm^{-1} due to this bending [26]. The weak band at 1260 cm^{-1} and the medium band at 954 cm^{-1} in the IR spectrum are assigned to the wagging and rocking deformation modes respectively of the methylene group.

3.3. Thermal studies

The TG and DTG curves of the sample are depicted in Fig. 8 and the DSC curve in Fig. 9. Muraishi *et al.* [27] have reported the thermal decomposition of the compound in different atmospheres. A close examination of the curves in the present case shows that all the transformations are associated with mass changes. The mass loss in the first stage (92–250°C) corresponds to dehydration process. In the DSC curve, an endothermic peak is seen at 158°C and another one at 192°C. This makes it evident that the dehydration proceeds via two steps. Each of these corresponds to a loss of one water molecule. The DSC curve also shows that one of the water molecules is more tightly bonded than the other, since the energies involved in the two steps are different. The observed mass loss of 21.14% in the dehydration process is in close match with the calculated value of 20.20%.

The second stage is associated to the decomposition of the anhydrous malonate yielding calcium carbonate. This happens in the temperature range 345–495°C. The observed mass loss of 24.36% in this process is in agreement with the calculated value of 23.60%.

The third and final stage in the thermogram shows a mass loss of 25.51% as against the calculated value of 24.72%. The DTG curve shows the corresponding peak at 764°C. This stage corresponds to the formation of calcium oxide from calcium carbonate by eliminating carbon dioxide. The results are in agreement with those reported by Muraishi *et al.* However, the temperatures of dehydration and decomposition in the present case are higher. This can be attributed to the flawless crystalline nature of the samples produced by this technique.

The overall decomposition reaction of the material could be satisfactorily represented as follows, which also gives a good stoichiometric balance.

$$CaC_3H_2O_4{\cdot}2H_2O \xrightarrow{(92-175^\circ C)} CaC_3H_2O_4{\cdot}H_2O + H_2O$$

$$CaC_3H_2O_4{\cdot}H_2O \xrightarrow{(175-250^\circ C)} CaC_3H_2O_4 + H_2O$$

$$CaC_3H_2O_4 + 2O_2 \xrightarrow{(345-495^\circ C)} CaCO_3 + 2CO_2 + H_2O$$

$$CaCO_3 \xrightarrow{(625-800^\circ C)} CaO + CO_2$$

4. Conclusions

Crystals of calcium malonate hydrate were obtained by gel-aided solution technique, by combining the advantages of solution growth and gel growth methods. All the crystals were formed initially in the upper solution, near the interface. Lower concentrations of the nutrients as well as lower gel densities favoured the formation of transparent and well faceted crystals. Also neutral or slightly acidic gel column was able to produce reasonably good crystals. The age of the gel had practically no impact on the growth kinetics. The XRD pattern indicates that the material grown by this route has the same structure as prepared by other methods. Spectral study of the sample shows the presence of crystallographically inequivalent water molecules with hydrogen bonds in the structure. It also shows strong atomic bonding in the carboxylate group. The thermal decomposition pattern of the material suggests three-stage decomposition and the DSC curve confirms the presence of two types of water molecules in the crystal lattice. The water of crystallization is completely lost well before the onset of anion decomposition. As expected for metal-organic compounds, the sample reduces to the metal oxide, at 764°C. From the experimental studies it has been observed that gel-aided solution technique can be successfully harnessed for the preparation of quality crystals of calcium malonate hydrate.

Acknowledgements

The authors are thankful to the Regional Sophisticated Instrumentation Centre, Madras, for providing IR and LR facilities. Also one of the authors, P. A. Varughese, is grateful to the University Grants Commission, Government of India, for the award of a fellowship under the IX plan.

References

1. A. COSTA-BAUZÁ, F. GRASES and O. SÖHNEL, *Cryst. Res. Technol.* **28** (1993) 337.
2. H. K. HENISCH, J. DENNIS and J. I. HANOKA, *J. Electrochem. Soc.* **112** (1965) 627; *Phys. Chem. Solids* **26** (1965) 493.
3. E. S. HALBERSTADT and H. K. HENISCH, *J. Cryst. Growth* **34** (1968) 363.
4. P. SELVARAJAN, B. N. DAS, H. B. GON and K. V. RAO, *J. Mater. Sci. Lett.* **12** (1993) 1210.
5. C. MEDRANO, P. GÜNTER and H. AREND, *Phys. Status Solidi* **14B** (1987) 749.
6. N. NAKATANI, *Jpn. J. Appl. Phys.* **30** (1991) 1961.
7. S. MAGNUSSON, L. SOTTRUP-JENSEN, T. E. PETERSON, H. R. MORRIS and A. DELL, *FEBS Lett.* **44** (1974) 189.
8. J. STENFLO, P. FERNLUND, W. EGAN and P. ROEPSTORFF, *Proc. Natl. Acad. Sci., USA* **71** (1974) 2730.
9. F. G. PRENDERGAST and K. G. MANN, *J. Biol. Chem.* **252** (1977) 840.
10. J. B. LIAN, P. V. HAUSCHKA and P. M. GALLOP, *Fed. Proc.* **37** (1978) 2615.
11. M. R. CHRISTY, R. M. BARKLEY, T. H. KOCH, J. J. VAN BUSKIRK and W. M. KIRSCH, *J. Amer. Chem. Soc.* **103** (1981) 3935.
12. A. ZELL, H. EINSPAHR and C. E. BUGG, *Biochem.* **24** (1985) 533.
13. R. C. MEHROTRA and R. BOHRA, "Metal Carboxylates" (Academic Press, London, 1983) p. 318.
14. K. RAJENDRABABU, M. DEEPA, C. M. K. NAIR and V. K. VAIDYAN, *Cryst. Res. Technol.* **32** (1997) 733.
15. G. VARGHESE and M. A. ITTYACHEN, *J. Mater. Sci. Lett.* **13** (1994) 1729.
16. G. VARGHESE, M. A. ITTYACHEN and J. ISSAC, *Cryst. Res. Technol.* **25** (1990) 153.
17. H. K. HENISCH, "Crystals in Gels and Leisegang Rings" (Cambridge University Press, 1986).
18. E. V. BRUSAU, G. E. NARDA, J. C. PEDREGOSA, G. ECHEVERRIA and G. M. PUNTE, *J. Solid State Chem.* **143** (1999) 174.
19. L. J. BELLAMY, "The IR Spectra of Complex Molecules," Vol. 1 (Chapman and Hall, London, 1975).
20. K. NAKAMOTO, "IR and Raman Spectra of Organic and Coordination Compounds," 5th ed. (Wiley, New York, 1977).
21. J. T. EDSALL, *J. Chem. Phys.* **5** (1937) 508.
22. V. P. MAHADEVAN PILLAI, V. U. NAYAR and V. B. JORDANOVSKA, *J. Solid State Chem.* **133** (1997) 407.
23. M. J. SCHMELZ, I. NAKAGAWA, S. MIZUSHIMA and J. V. QUAGLIANO, *J. Amer. Chem. Soc.* **81** (1959) 287.
24. K. NAKAMOTO, Y. MORIMOTO and A. E. MARTELL, *ibid.* **83** (1961) 4528.
25. N. GUTMAN, B. MÜLLER and H. TILLER, *J. Solid State Chem.* **119** (1995) 331.
26. M. KEMICHE, P. BECKER, C. CARABATOS-NÉDELEC, B. WYNCKE and F. BRÉHAT, *Vib. Spectrosc.* **11** (1996) 135.
27. K. MURAISHI, Y. SUZUKI and Y. TAKAHASHI, *Thermochim. Acta* **286** (1996) 187.

Received 29 July 2002
and accepted 29 April 2004